



City Research Online

City St George's, University of London

Citation: Brücker, C., Schnakenberg, U., Rockenbach, A. & Mikulich, V. (2017). Effect of Cilia Orientation in Metachronal Transport of Microparticles. *World Journal of Mechanics*, 07(01), pp. 1-10. doi: 10.4236/wjm.2017.71001

This is the accepted version of the paper.

This version of the publication may differ from the final published version. To cite this item please consult the publisher's version.

Permanent repository link: <https://openaccess.city.ac.uk/id/eprint/21330/>

Link to published version: <https://doi.org/10.4236/wjm.2017.71001>

Copyright and Reuse: Copyright and Moral Rights remain with the author(s) and/or copyright holders. Copies of full items can be used for personal research or study, educational, or not-for-profit purposes without prior permission or charge, unless otherwise indicated, provided that the authors, title and full bibliographic details are credited, a hyperlink and/or URL is given for the original metadata page and the content is not changed in any way. For full details of reuse please refer to [City Research Online policy](#).

EFFECT OF CILIA ORIENTATION IN METACHRONAL TRANSPORT OF MICROPARTICLES*

Christoph Brücker¹, Uwe Schnakenberg², Alexander Rockenbach², Vladimir Mikulich³

¹ Department of Mechanical Engineering and Aeronautics, City University London, UK

² Institute of Materials in Electrical Engineering 1, RWTH Aachen University, Germany

³ Institute of Mechanics and Fluid Dynamics, TU Bergakademie Freiberg, Germany

Email: christoph.bruecker@city.ac.uk

How to cite this paper: Author 1, Author 2 and Author 3 (2016) Paper Title. ***** *, *.*.

http://dx.doi.org/10.4236/****.2016.*****

Received: **** **, **

Accepted: **** **, **

Published: **** **, **

Copyright © 2016 by author(s) and Scientific Research Publishing Inc. This work is licensed under the Creative Commons Attribution International License (CC BY 4.0).

<http://creativecommons.org/licenses/by/4.0/>



Open Access

Abstract

A biomimetic approach is developed which generates a directed transversal transportation of micron-sized particles in liquids based on the principle of cilia-type arrays in coordinated motion. Rows of flaps mimicking planar cilia are positioned off-centre along an array of cavities covered with membranes that support the flaps. These membranes are deflected from a concave to a convex shape and vice versa by pneumatic actuation applying positive and negative pressures (relative to the ambient) inside the cavities. As a result, the off-center positioned flap on top of the membrane tilts to the left or right within such a pressure cycle, performing a beat stroke. Since each cavity can be addressed in the device individually and in rapid succession, waves of coordinated flap motion can be run along the wall. Such travelling waves are generated and transport of particles along the cilia surface is achieved in both symplectic and antiplectic direction. The initial tilt of the flaps relative to the wall-normal direction is of importance for the transport direction.

Keywords

Cilia transport, metachronal wave, fluidic transport, micro-particles

1. Introduction (Heading 1)

Thanks to the advances in micro- and nanofabrication technologies during the last decades several micro-manipulation techniques offer the possibility to transport and rotate individual micro-particles or micro-parts. Sorting, trapping, separation, aligning, concentration, patterning, focusing, merging, delivery, and (self-)assembly of micro-objects are of special interest in basic research, development and industrial relevant applications. Different manipulation principles, such as trapping by optical tweezers [1], gripping techniques [2-5], ultrasonic [6,7] or magnetic actuation [8] as well as the use of capillary and electrostatic forces for self-assembly of parts [9] are reviewed in detail. The manipulation

**Special description of the title. (dispensable)

of particles in microfluidic devices using electrical fields are carried out by electrophoresis or dielectrophoresis actuation principle [10,11].

When looking to nature, ciliated surfaces are found for transport purposes, such as in the respiratory tract [12] or the fallopian tube [13] or are used for self-propelling of micro-swimmers [14]. Ciliated walls actuated by applying metachronal waves can be perfectly used for particle transport. The interaction between the particles, the liquid layer and the cilia is coupled by friction at the contacting surfaces, viscous drag and inertia, depending on the local Reynolds number of the cilia beat and the flow around the particles. This raises the question of the effectiveness of metachronal coordination not only for transport of any liquid surrounding the cilia but also for transport of particles itself submerged within the liquid [15] or in contact with the cilia tips. Momentum transfer is possible by direct contact between the particles and the cilia. Different artificial cilia models are already developed to investigate and characterize the transport behaviour near the ciliated wall [16-26].

The method presented herein uses micro-structured surfaces with arrays of artificial cilia that are individually micro-pneumatically activated [26]. We used spherical micro-particles with a diameter larger than the spacing between the artificial cilia and studied their transport behaviour when metachronal waves running along the ciliated wall are applied. Two different positions of the cilia in rest conditions were studied: the first with the cilia protruding into the liquid at an axis perpendicular to the wall and the second with a pre-defined tilt.

2. Methods

2.1. Design concept

The principle described is to generate coherent transport of spherical particles along a wall covered with artificial cilia, called flaps. The design concept is based upon a model built for liquid flow studies along flexible walls, as illustrated in Figure 1.

It consists of a pneumatic drive system to generate the movement of flaps in arrays on top of a transportation device, henceforth referred to as port. The port has a total length of 80 mm and is milled from aluminium. On the surface of the port an array of 20 cavities (spacing Δs between each cavity is 1mm) made from PDMS (poly(dimethylsiloxane)) is located, each one covered with a flexible membrane. Each membrane has a flap on top of it (height 500 μm , thickness 50 μm , extension of the flap span in direction normal to the paper-plane 30 mm) which protrudes into the liquid layer at a defined angle relative to the membrane. The flap orientation at ambient pressure (planar membrane) is either perpendicular as in modification 1 or tilted at 45° as in modification 2, see Figure 1. The port houses pneumatic connectors on its bottom for the attachment of pneumatic tubes. These tubes deliver either positive or negative pressure (relative to the ambient) to each cavity

which is switched by magnetic valves. The ground state in the experiments is when negative pressure is applied to the cavities, and then all membranes are in concave state. A change in pressure from negative to positive in one cavity results in change of the curvature of the membrane from the concave state to the convex state. This causes the local flap to tilt to the right, performing a beat stroke. When the valve switches back to the ground state the flap relaxes back to its original position. The control of all 20 flaps to beat in metachronal wave-like pattern is explained further below.

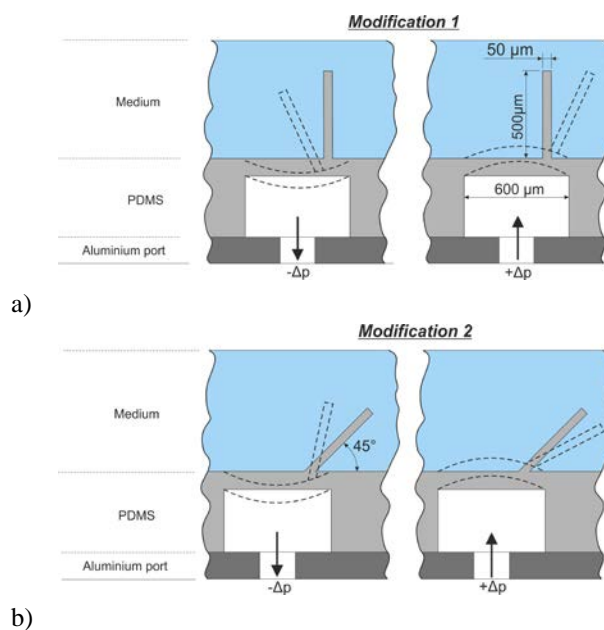


Figure 1. Schematic of the pneumatic flap actuation mechanism in two modifications of the flaps. The solid contours represent the state at ambient pressure $\Delta p = 0$ where the membrane is flat. The dashed lines display the state of the membrane and the flap at the different pressure conditions at $\pm \Delta p \neq 0$. a) flaps have at $\Delta p = 0$ a tilt of 90° against the membrane; b) flaps have at $\Delta p = 0$ a tilt of 45° against the membrane. The flap angle can be adjusted in the manufacturing process of the membrane.

2.2. Experimental set-up

For the particle transport studies the port is integrated in an open oval channel at the bottom wall, see Figure 2. The open channel is 10 mm deep and is made of aluminum. It consists of two straight parts connected by semi-circular arches. Transparent glass windows are implemented into the sides of the channel walls to allow optical access with a high-speed camera (HS-C2 in figure 3). An optional second camera can look via a 45° prism from top onto the ciliated wall (HS-C1 in figure 3). The cameras are synchronized with each other while recording. Illumination is done with a LED-lighting system.

The drive and control unit to generate the metachronal waves is depicted in Figure 3. To

control the movement of every flap individually via the pneumatic system, a rail of 20 valves is used with the abovementioned pneumatic tubes connected to the port cavities. On one side the valves are connected to a pressurised air supply (positive pressure supply) and on the other side the valves are connected to a vacuum pump (negative pressure supply). The positive and negative relative pressures are monitored with two separate manometers. A Personal Computer with an analogue input/output controller (cRIO National Instruments) is used to trigger the valves. The controller has its own processor and a reconfigurable Field Programmable Gate Array (FPGA). The latter ensures that the execution of the control algorithms occurs in real-time. An additional amplifier is needed to amplify and transfer the signal to each valve.

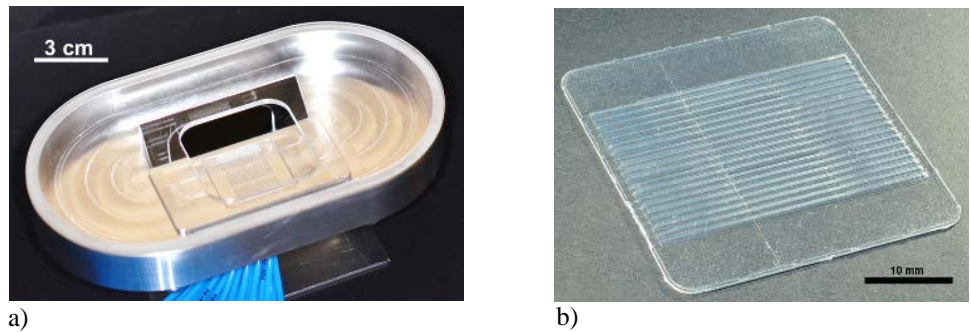


Figure 2. a) Closed-loop flow chamber. The silicon device glued to the connector is integrated into the chamber. The channels under the membrane are connected to the blue pressure tubes. b) Photograph of the upper membrane with the 20 transparent flaps arranged in rows with a spacing of $\Delta s = 1\text{mm}$.

The design concept has the following parameters to generate a particular form of meta-chronal waves: the wavelength which is equal to the pulse repetition length L along the flap array, the pulse propagation speed U and the number of neighbouring cavities which are active in a single pulse. This is visualised in Figure 4. Once the wave reaches the end, it is reintroduced at the beginning of the array. The time the valves need to switch from negative pressure to positive one and vice versa is approximately 4 ms. In comparison, for the flap it takes about 40 ms to move from one side to the other in such a pressure pulse. This is the consequence of the damping in the pressure lines which cause a delay of the pressure built up or decay under the membrane until it reaches the maximum or minimum value [26]. In the following, this period is referred as the characteristic beating time of a flap t_B . Another time-scale is attributed to the wave-cycle time T (inverse of the wave repetition frequency) which is the time between successive pulses at the same cavity and reads $T=L/U$.

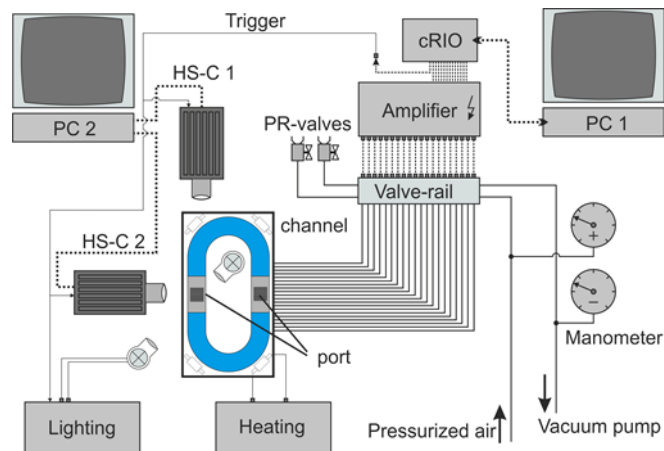


Figure 3. Schematic block diagram of the control and data acquisition setup, with a detailed view of the pneumatic design concept.

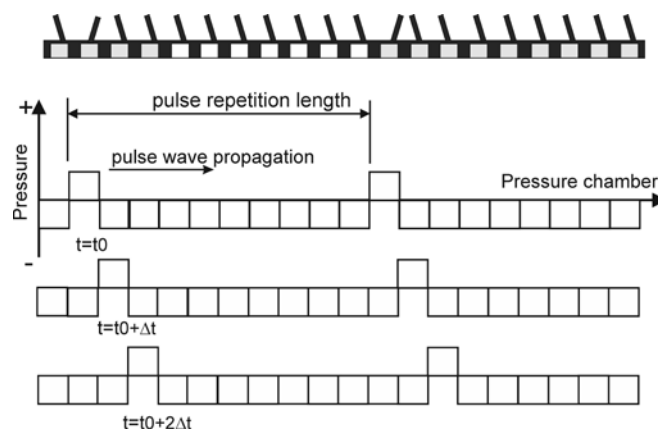


Figure 4. Principle of the wave generation with the controlled switching of the pressures in the cavities below the array of flaps. The propagation direction is from left to right. In the picture, the number of active cavities in a single pulse is the minimum of one. There is also the possibility to activate two or three neighbouring cavities to participate in a pulse. The flaps corresponding to the pulse are called the “active” flaps. The pulse pattern progresses through the array in time steps of Δt .

2.3. Experimental procedure

For all tests, the channel is filled with distilled water. It is held at a temperature of 24 °C. To be certain of an equal temperature distribution the channel, water and ports were monitored with an infrared camera. The water layer thickness was kept at 3 mm throughout all experimental procedures. Although two ports with different modifications respectively

are mounted in the channel, only one is used herein. Spherical polyamide particles with a density of 1.14 g/cm³ are used in the experimental procedure. The diameter was chosen to 2 mm to ensure that the particles do not fall into the gap between the flaps and remain in contact with their tips. The available spherical polyamide particles are coloured in white first to achieve a good visibility in the recordings. To detect any rotational movement, their surfaces were marked with irregular black dots in a second step. For each test the particles were carefully placed between the first and second flap on one side of the array. The template is used to format your paper and style the text. All margins, column widths, line spaces, and text fonts are prescribed; please do not alter them. You may note peculiarities. For example, the head margin in this template measures proportionately more than is customary. This measurement and others are deliberate, using specifications that anticipate your paper as one part of the entire journals, and not as an independent document. Please do not revise any of the current designations.

The test series were conducted with an applied pressure of 0.4 bar in positive and negative direction relative to the ambient pressure. Initial parametric studies have shown that at least ± 0.2 bar pressure has to be applied to the flaps to ensure the transport of the particles. At lower pressures, the momentum transferred to the particles is not sufficient to move the particles from one flap to the next.

3. Results

The focus of our studies is the transport process for the two different flap orientations. The difference between both settings is explained in Figure 1. The particle transport in general depends on a large set of parameters such as the Reynolds number of the flow around the particles, the density ratio between particle and fluid, the pulse pattern and wave speed as well as the shape and size of the particles. A study of all parameters is beyond the scope of the paper; rather we selected characteristic results to demonstrate the impact of cilia orientation on the transport direction under otherwise constant conditions.

3.1. Symplectic transport

Figure 5 shows the symplectic transport of the sphere with the flap modification 1 (flap orientation perpendicular at ambient pressure) when the pressure pulse propagation is applied from left to right. The beat cycle is when the flap tip rotates from left to right in clock-wise direction (red position in Figure 5) and relaxes back passing the blue state in Figure 5 until it ends again at the original state (black position in Figure 5). In the symplectic transport, the momentum transfer occurs mainly via a contact between the sphere and the side wall of the flap. The major phase in momentum transfer is the forward-directed stroke of the flap. The greater contact area allows a more efficient horizontal transportation, resulting in a high particle velocity of 12 mm/s. Furthermore, the sphere gets a positive spin. Overall, the sphere leads the front crest of the travelling wave and is as fast as the wave speed is. Note that reversing the

propagation direction from right to left does not lead to a transport at all.

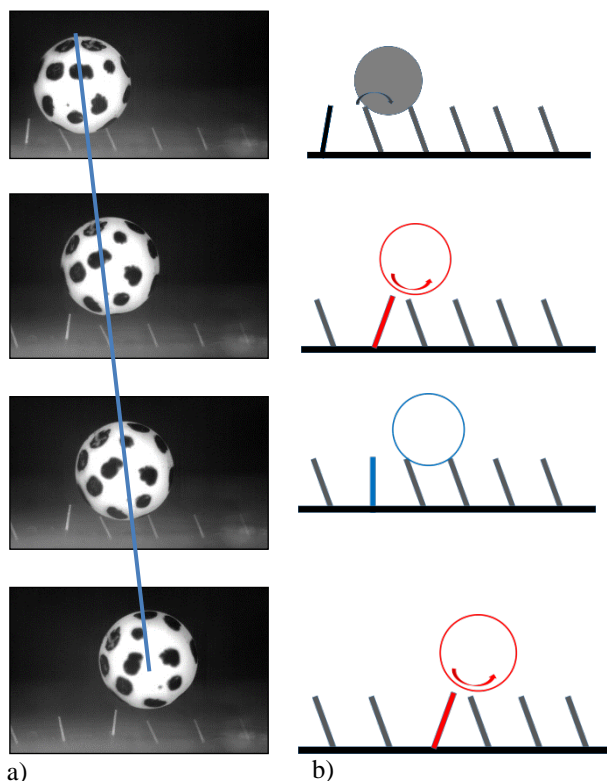


Figure 5. Symplectic transport of a sphere along the ciliated wall. Pulse propagation is from left to right at a speed of $12 \Delta s/\text{sec}$ ($12 \text{ mm}/\text{sec}$). Mean particle speed in transport direction $U_p=U$ is equal to wave propagation speed. Spin of the particle is counter-clockwise. Number of active flaps in a pulse is one.

3.3. Antiplectic Transport

In comparison, Figure 6 shows an example where an antiplectic transport is observed for flap modification 2 (flap tilted by 45° at ambient pressure). Note that for these experiments the pressure pulse propagation is from the right to the left and was set to the same velocity as in the experiments with flap modification 1. In this case, the number of active flaps involved in the momentum transfer was increased to two, which gave the best results for transport. The beat cycle leads to the simultaneous tilt of two neighboring flaps which are in contact with the sphere. The tilt causes the sphere to move to the right down into the gap on the right-hand side of the flap activated in the previous beat. This is because the latter is relaxing to its original position. Within this motion phase of the sphere the right-hand sided active flap is starting to relax back which supports the further motion in combination with the additional impact of a negative spin. This causes the sphere to roll over to the tip of the flap to the next gap on the right-hand side. In this way, the

sphere is shifted a distance of Δs per wave cycle in direction counter to the wave propagation. Again, a reversal of the propagation direction from left to right does not show a transport at all for this configuration.

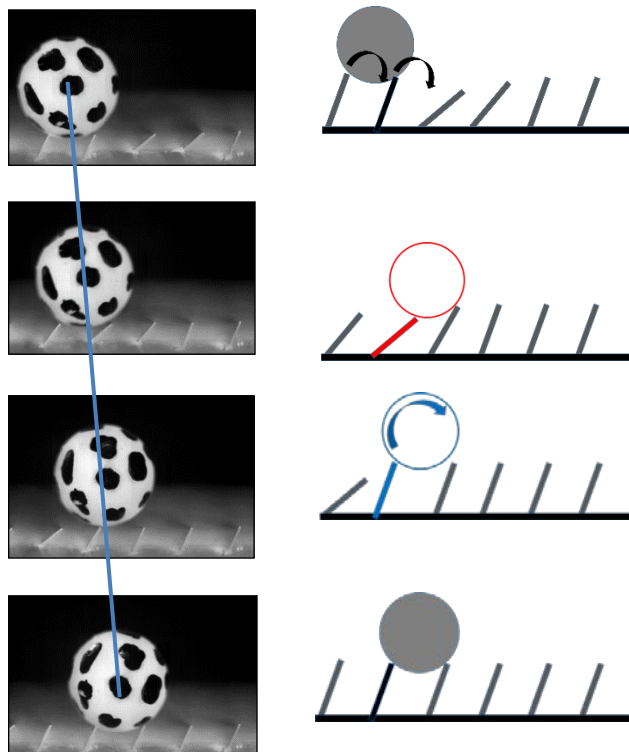


Figure 6. Antiplectic transport of a sphere along the ciliated wall. Pulse propagation is from right to left at a speed of $12 \Delta s/\text{sec}$ ($12 \text{ mm}/\text{sec}$). Mean particle speed in transport direction is $U_p = \Delta s/T$ which is one flap per wave cycle. Spin of the particle is clockwise. Number of active flaps in a pulse is two.

A successful transport depends primarily on the momentum transfer of the flaps onto the particle and the moving pattern of the waves. It is crucial for maximum transport velocity how the particles are positioned before they receive the impulse and in which manner the particles travel after receiving the impulse. A logical pattern is a shift of one flap per beat cycle so that the next flap takes over the sphere and pushes it further forward. In this case the transport is symplectic and reaches maximum speed. However, symplectic transport requires an initial pre-tilt of the flaps against the wave propagation direction as shown in Figure 1 for the initial situation (negative pressure), otherwise the transport does not happen. If the direction of the pre-tilt is changed but the beat direction is kept the same, the transport is only observed if the wave propagation direction is reversed. This means that the observed configuration leads to an antiplectic transport.

4. Conclusion

The transportation of particles along ciliated walls is of highly complex nature. In order to simplify the parameter space an artificial ciliated wall system is designed which allows us to study the transport of selected particles under defined beating conditions. As reference, we selected spherical particles of slightly higher density than the carrier liquid water. In addition, their diameter is larger than the spacing between the flaps to ensure contact with the flap tips. The results show that the pre-tilt and orientation of the flaps is an important parameter which decides about the transport direction.

Acknowledgements

Funding is given by the Deutsche Forschungsgemeinschaft (DFG) under grant BR 1494/30-1 (AOBJ 622417) and SCH 587/15-1 within priority program SPP 1726 “Microswimmers”. Funding of the position of Professor Christoph Bruecker as the BAE SYSTEMS Sir Richard Olver Chair in Aeronautical Engineering is gratefully acknowledged herein.

References

- [1] Grier DG 2003 A revolution in optical manipulation *Nature* **242** 810-6
- [2] Cecil J *et al* 2007 Assembly and manipulation of micro devices – A state of the art survey *Robotics and Computer-Integrated Manufacturing* **23** (5) 580-8
- [3] Vasquez D *et al* 2007 A review of gripping and manipulation techniques for micro-assembly applications *Int. J Production Research* **43** (4) 819-28
- [4] Ouyang PR *et al* 2006 Micro-motion devices technology: The state of arts review *Int J Adv Manu Technol* **38** (5) 463-78
- [5] Gauthier M *et al* 2006 Analysis of forces for micromanipulation in dry and liquid media *J Micromechatronics* **3** (3) 389-413
- [6] Drinkwater BW 2016 Dynamic-field devices for the ultrasonic manipulation of microparticles *Lab Chip* DOI: 10.1039/c6lc00502k
- [7] Destgeer G *et al* 2015 Recent advances in microfluidic actuation and micro-object manipulation via surface acoustic waves *Lab Chip* **15** 2722-38
- [8] Gijs MAM 2004 Magnetic bead handling on-chip: new opportunities for analytical applications. *Microfluid Nanofluid* **1** 22-40
- [9] Mastrangeli *et al* 2009 Self-assembly from milli- to nanoscales: methods and applications *J Micromech Microeng* **19** 083001
- [10] Pethig R 2010 Review article – Dielectrophoresis: Status of the theory, technology and applications *Biomicrofluidics* **4** 022811
- [11] Velev OD *et al* 2009 Particle-localized AC and DC manipulation and electrokinetics *Annu Rep Prog Chem, Sect. C* **105** 213-46
- [12] G.R. Fulford GR *et al* 1986 Muco-ciliary transport in the lung. *J Theor Biol* **121** 381-402
- [13] Lyons RA *et al* 2006 The reproductive significance of human Fallopian tube cilia *Human Reproduction Update* **12** (4) 363-72
- [14] Elgeti J *et al* 2015 Physics of Microswimmers – single particle motion and collective behaviour: a review *Rep Prog Phys* **78** 056601
- [15] Masoud H *et al* 2011 Harnessing synthetic cilia to regulate motion of microparticles *Soft Matter* **7** 8702-8
- [16] den Toonder JM *et al* 2008 Artificial cilia for active micro-fluidic mixing *Lab Chip* **8** (4) 533-41
- [17] den Toonder MJM *et al* 2013 Microfluidic manipulation with artificial/bioinspired cilia *Trends Biotechnol* **31** (2) 85-91
- [18] Khaderi SN *et al* 2011 Magnetically-actuated artificial cilia for microfluidic propulsion *Lab Chip* **11** (12) 2002-10
- [19] Shields AR *et al* 2010 Biomimetic cilia arrays generate simultaneous pumping and mixing regimes *Proc Natl Acad Sci* **107**, (36) 15670-5

- [20] Fahmi F *et al* 2009 Micro-fluidic actuation using magnetic artificial cilia *Lab Chip* **9** (23) 3413–21 Dec.
- [21] Timonen JVI *et al* 2010 A facile template-free approach to magnetodriven, multifunctional artificial cilia. *ACS Appl Mater Interfaces* **2** (8) 2226–30
- [22] van Oosten CL *et al* 2009 Printed artificial cilia from liquid-crystal network actuators modularly driven by light *Nat Mater* **8** (8) 677–82
- [23] Zarzar LD *et al* 2011 Bio-inspired design of submerged hydrogel-actuated polymer microstructures operating in response to pH *Adv Mater* **23** (12) 1442–6
- [24] Sanchez T *et al* 2011 Cilia-like beating of active microtubule bundles *Science* **333**, (6041) 456–9
- [25] Dayal P *et al* 2012 Chemically-mediated communication in self-oscillating, biomimetic cilia *J Mater Chem* **22** (1) 241, 2012.
- [26] Rockenbach A *et al* 2015 Fluid transport via pneumatically actuated waves on a ciliated wall. *J Micromech Microeng* **25** 125009